



Technical Document

Frequency response of a real cable network and its impact on field PD measurements

S. A. Madhar, P. Mraz, S. B. Pereira, N. Akroud

TD-110



HAEFELY

Current and voltage – our passion

FREQUENCY RESPONSE OF A REAL CABLE NETWORK AND ITS IMPACT ON FIELD PD MEASUREMENTS

Saliha Abdul Madhar
Haefely Test AG –Switzerland
TU Delft –the Netherlands
smadhar@haefely.com

Petr Mráz
Haefely Test AG – Switzerland
pmraz@haefely.com

Sonia Barrios Pereira
Ormazabal - Spain
sbp@ormazabal.com

Nabil Akroud
Ormazabal – Spain
nak@ormazabal.com

ABSTRACT

Asset condition monitoring through Partial Discharge (PD) measurements is widely used for pre-emptive maintenance especially in cable networks. Several monitoring systems rely on measurements in the High Frequency (HF) band using wideband sensors when it comes to PD monitoring to have higher Signal to Noise Ratios (SNR), ignoring the radical attenuation of the higher frequencies by the cable. This paper presents measured values of attenuation from measuring loops and several other important insights that can help in the interpretation of PD measured data.

INTRODUCTION

On-line monitoring of Partial Discharges (PD) is a widely used maintenance technique for cable networks. This is because the physical structure of the cable is a coaxial waveguide that poses as a one dimensional medium for the discharge pulse propagation; which in turn provides the added advantage of pulse/defect localization. However, none of the distribution cable networks comprise purely of cables, they include joints, interconnectors, switchgears, busbar etc. These components pose as a discontinuity in the path of the travelling PD pulse leading to complex phenomenon of pulse reflections, refractions and radiation. Several monitoring systems rely on measurements in the High Frequency (HF) band [1] using wideband sensors when it comes to PD monitoring to have a higher SNR, ignoring the radical attenuation of the higher frequencies by the cable [2]. This paper presents two important assessments associated with PD measurements on real cable networks. Firstly, this paper provides the values of measured attenuation and limits of measurement when it comes to PD measurements in general. It demonstrates the damping of the high frequencies merely by the influence of the measuring loop inductance. Second, it presents the measurement results from an actual MV cable network showing pulse propagation in various network configurations measured using Haefely's DDX 9121b PD detector.

PULSE ATTENUATION

The propagation of the partial discharge through the measuring loop alone causes severe attenuation of the pulse's high frequencies. This is because the cables (both power cables and measuring cables) are built for lower frequencies [3]. In order to demonstrate this phenomenon

a series of precise measurements are performed on cables used for interconnection of HV components such as the RG58 and unshielded banana cables. Fig.1 shows the measured values of attenuation (dB/m) and phase velocity (m/s) for a RG58 cable based on Eq.1 [4]. It can be noted that the value of pulse attenuation is frequency dependant and increases with increasing frequencies.

$$H_{meas} = V_r(\omega)/V_i(\omega) = e^{-\gamma^2 l c} \quad \text{Eq.1.}$$

Fig.2 presents the losses over a 2 m long RG58 coaxial cable versus a banana cable which exhibits a dramatic difference at higher frequencies.

It clearly demonstrates that for PD measurements it is clearly more advantageous to use coaxial connections using BNC/SMA connectors instead of making long and lossy banana connections.

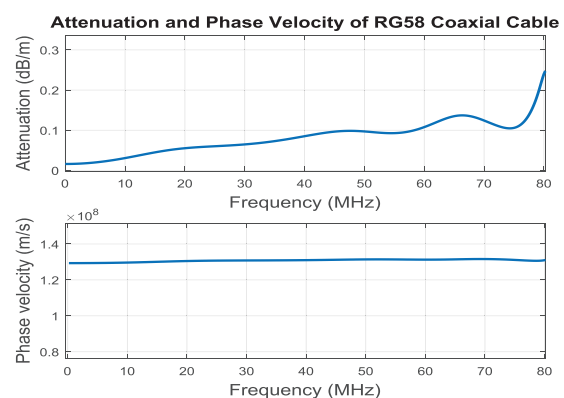


Fig.1. Measured values of attenuation and phase velocity of a RG58 cable in dB/m.

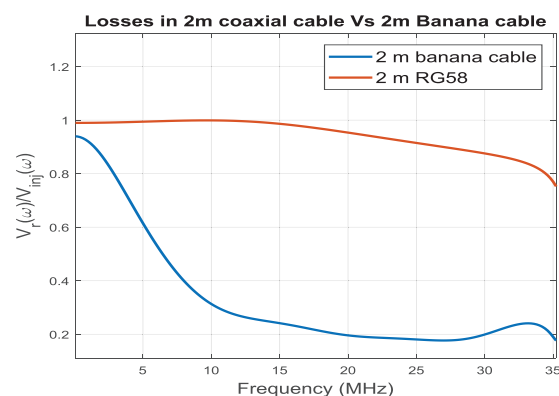


Fig.2. Loss measurement in p.u for a 2 m RG58 coax Vs a banana connection.

Next, the performance of the capacitors is measured using a Vector Network Analyser (VNA) which makes a frequency sweep of a constant amplitude sine wave across its 2 S-ports. Then, using the series-through method the impedance of the test object can be calculated. It is important to note here that the impedance of the capacitor can never be measured ideally without stray influences. From the size of the capacitor (through which current flows) arises a certain value of inductance (stray) based on the shortest current loop connected across it. Therefore, this measurement per se measures the capacitance of the test object and the inductance of the shortest test loop that can possibly be made over the capacitor. The test was repeated for 3 different capacitor units: 10 kV, 100 kV and 200 kV of heights 10 cm, 75 cm and 1.5 m respectively, using short cable length and using 10 m long cable. The results of the test are consolidated into a single graph for comparison and presented in Fig.3. The resonant frequencies follow certain trends as listed below:

- The resonant frequency of 1nF capacitor is greater than that of 10 nF ($f_r = \frac{1}{2\pi\sqrt{LC}}$)
- $f_{r,10\text{ kV}} > f_{r,100\text{ kV}} > f_{r,200\text{ kV}}$ (different heights)
- $f_{r,short\ loop} > f_{r,10\ m\ loop}$

The difference in the resonant frequencies of the 100 kV and the 200 kV capacitors arising from the difference in their sizes is visible in the measurement using the shortest loops. But once 10 m of cable is connected across their terminals these differences disappear. This is because earlier the loop sizes were: 3 m (200 kV cap.) and 1.5 m (100 kV cap.) which is a ratio of 2:1. After 10 m of cable is connected: 21.5 m (200 kV cap.) and 20.75 m (100 kV cap.) it yields a ratio of 1.036:1. So the loop sizes are almost a factor of 1 and not much change in the inductances arises from them as a consequence.

Therefore, it can be seen that typically for frequencies above 1 to 1.5 MHz, their performance becomes inductive. PD measurements cannot be made over the resonance frequencies due to undefined/unstable transfer impedance which makes the charge calibration invalid.

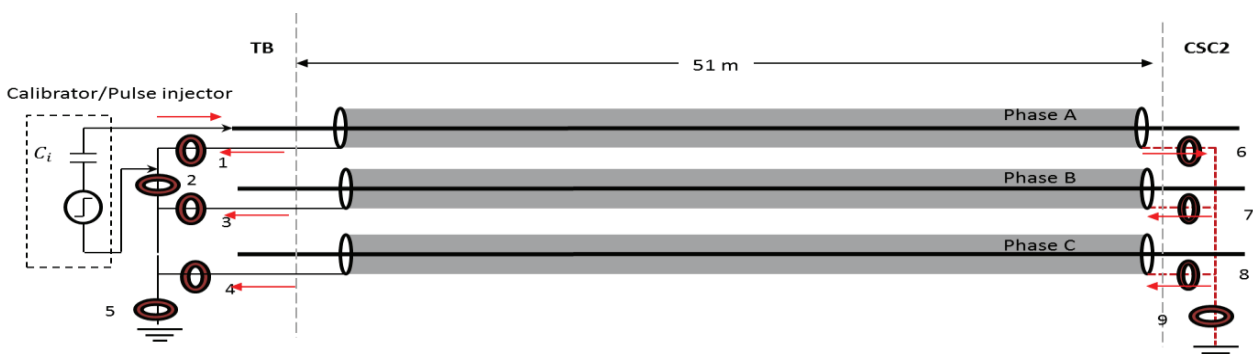


Fig.5. The measuring setup at the test bay of UDEX.

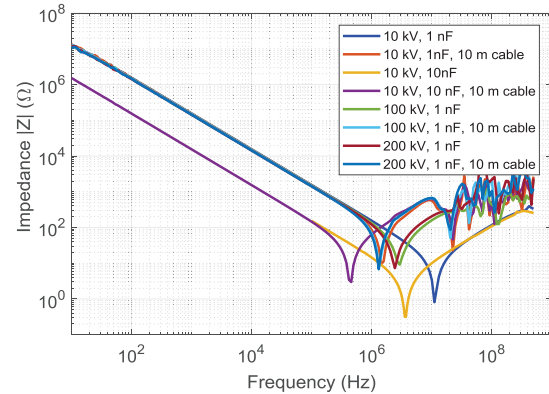


Fig.3. Impedance of capacitor units measured using the VNA.

Hence, this ascertains that PD measurements are more likely to be stable and inter-comparable when performed at lower frequencies (LFs) (< 1.5 MHz).

For instance, when calibrating a cable network at LFs (30 kHz to 900 kHz), though the real PD pulse attenuates during propagating from the PD source to the measuring point the error in charge measurement (in pC) is minor because the LFs are damped negligibly. However, the error is more appreciable while using wideband measurement, even though the SNR improves by several folds. One such example is shown in Fig.4.

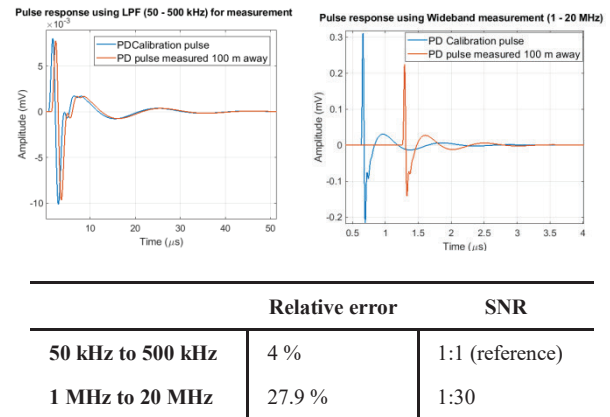


Fig.4. PD measurement using Low Frequency and High Frequency measurement.

MEASUREMENT ON MV CABLE NETWORK

3-phase coupling

This section shows the cross-coupling of the PD pulse to other phases when introduced in one phase. Fig.5 shows the schematic of the measurement setup. A fast pulse with a flat spectrum up to 25 MHz was used for injection. The pulse response was measured using High Frequency Current Transformers (HFCTs) with flat transfer impedance from 100 kHz to 19 MHz.

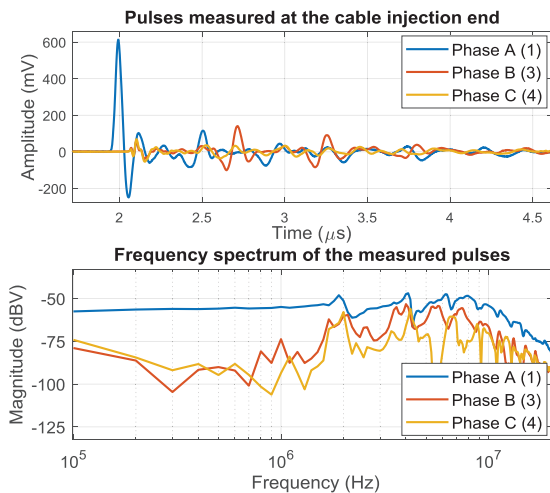


Fig.6. Pulses measured at the cable near end and their frequency spectrums (refer measurement points numbered in Fig.6)

Due to the short nature of the cable section (51 m) the pulse reflections cannot be seen clearly due to overlapping. However this information can be obtained from the respective frequency spectrum shown on Fig.6 which shows resonances at multiples of ~ 1.8 MHz which is the frequency of the standing wave in the cable section. This can be confirmed using the relation;

$$\text{Time of arrival of reflected pulse} = \frac{2l}{v}$$

$$\sim 550 \text{ ns (1.8 MHz)}$$

The ratio of the coupling from Phase A to Phases B and C is 1:30. This arises from the values of parasitic capacitance. It can also be noted from the frequency spectrum of the discharge pulse that the energy drastically reduces after 10 MHz (While the resonances begin at ~2 MHz) for a cable of 51 m in length. In order to give the reader an impression of the pulse energy after different propagating lengths the attenuation function of the cable is implemented in MATLAB based on [5], the pulse amplitudes and frequencies are presented in Fig.7.

This shows the drastic damping of the higher order frequencies (> 1 MHz) below -3 dB for distances over 500 m. This is one reason why IEC 60270 standards validate measurements between 30 kHz and 1 MHz only [6].

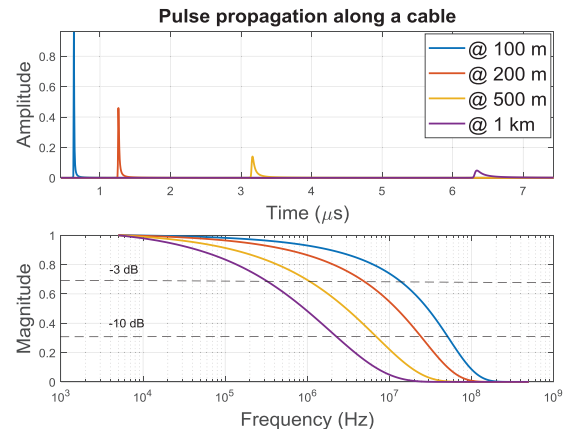


Fig.7. Pulse attenuation with propagation along the cable (all units are in p.u).

Case Study

A real defect was created on the cable network by disconnecting the ground connections of the cable termination in order to create a 'floating ground' defect. The measurements were performed using a coupling capacitor and a HFCT individually to allow a comparison between both cases.



Fig.8. Measuring setup installed on 3-phases.

Measurement using Coupling Capacitor

Once the whole circuit is closed, excluding the connection to supply, a final calibration is done at the test bay to check the frequency response of the complete line. But before selecting the frequency bandwidth for calibration the frequency spectrum of the noise is studied to determine if there are any unwarranted peaks that can be avoided. Fig.11 shows the calibration pulse spectrum with a flat nature from 100 kHz to 500 kHz over which calibration is performed. The discharge pulses measured on the 3 phases shown in Fig.9 alongside their frequency spectrums shows that the real discharge pulse has flat frequency characteristics over the calibration band thereby keeping the calibration valid [7]. The minimum sensitivity of detection is ~400 pC (considering noise and attenuation of line).

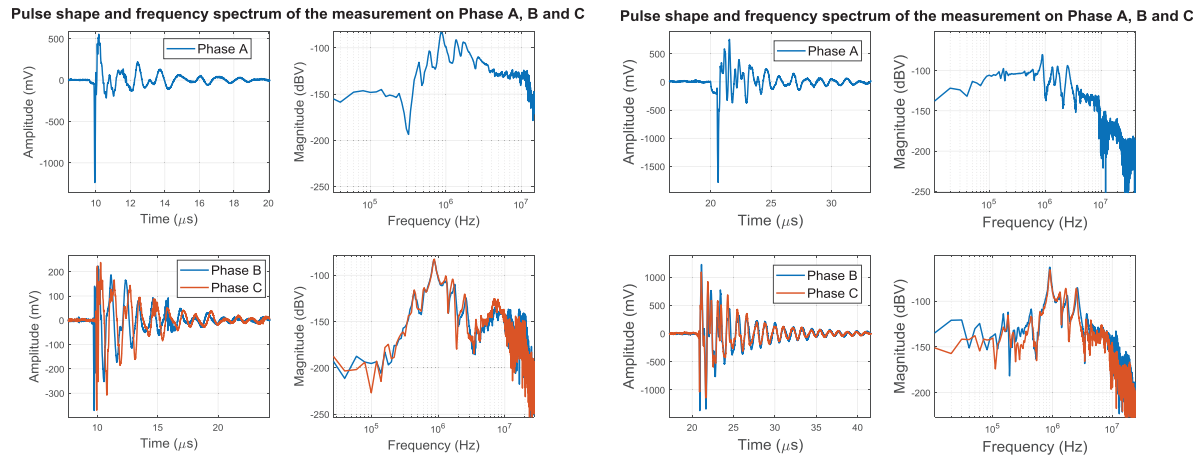


Fig.9. The frequency spectrum of the pulses as measured on (left) Phases A, B and C using coupling capacitor and (right) using HFCT.

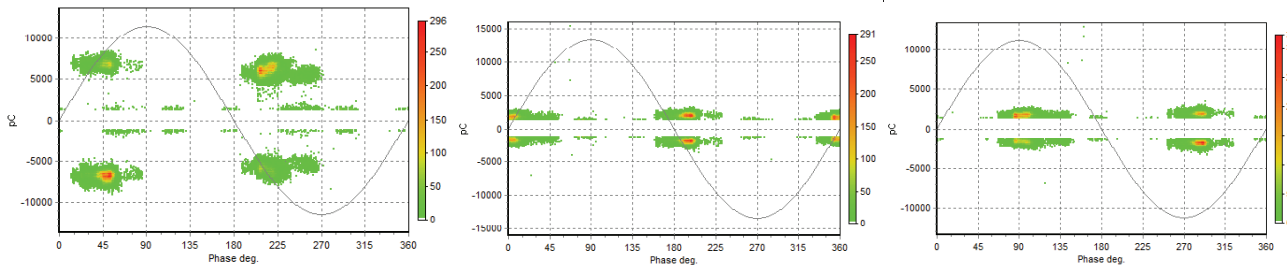


Fig.10.PRPD pattern of the defect measured using Coupling Capacitors.

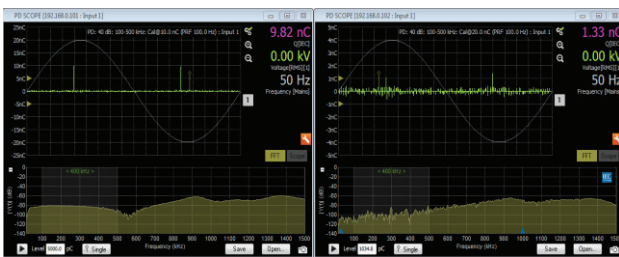


Fig.11.The calibration pulse and the spectrum of Phase A (left) and cross-coupling to Phase B (right) measured using the coupling capacitor.

The PRPD patterns recorded are shown in Fig.10. The phase with the largest PD amplitude denotes the defective phase. In addition, the pattern is also slightly phase shifted on the cross-coupled phases. When the individual pulse shape and polarity are visualized using the signal output of the DDX 9121b seen from Fig.9, the pulse on the defective phase has a polarity opposite to the pulse in the healthy phases.

Measurement using HFCT

The same measurement is repeated using the HFCT. The system is recalibrated, the new calibration spectrum is shown in Fig.12, and calibration is done between 200 kHz to 600 kHz to avoid the high noise at the LFs. It is

also beneficial to look at the cross-coupling on the other phases to keep it at a low value; this will help in recognition of the faulty phase. The real discharge pulses are displayed in Fig.9. The flat nature of the low frequency spectrum once again validates the calibration.

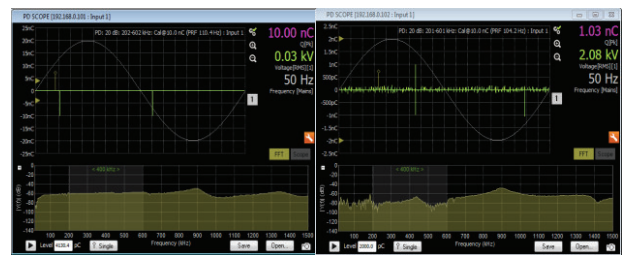


Fig.12.The calibration pulse and the spectrum of Phase A (left) and cross-coupling to Phase B (right) measured using the HFCT.

PD measurements can be done using several different sensor types. When done correctly they will all yield the same results. As observed, the pulse shapes measured using HFCT are different from the ones measured using coupling capacitor but this is only because of the difference in the measuring impedance in the 2 cases. However, the value of average charge in both cases is very similar.

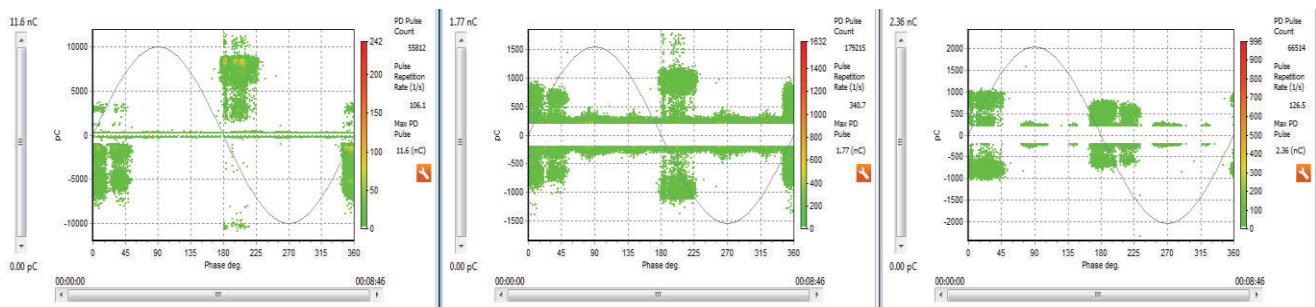


Fig.13.PRPD pattern of the defect measured using the HFCT.

Measuring using a wideband sensor such as the HFCT provides greater visibility in terms of PD detection. However, that does not necessitate correct measurement of the discharge in terms of magnitude (pC). In most cases measuring on the HF resonance peaks can make the data interpretation more complex as the measured amplitude on the healthy phases is similar to the defective phase as these resonance arise from the physical dimensions of the line.

CONCLUSION

This paper presents the challenges of measuring PD on an actual cable network. It explains sequentially the steps to be followed in order to not just detect the PD in a cable network but also measure it with reasonable level of accuracy.

As stated earlier, following the IEC standards allows inter-comparability of the measured values in terms of charge (pC). However, the stringent frequency requirements (lower frequency cut-off ≤ 100 kHz) may not be possible to fulfil while performing on-site measurements due to high noise/low sensitivity. Therefore, looking to the frequency spectrum of the pulse and measuring over the flat spectrum instead of resonances will preserve the validity of the calibration and make the measured values of charge reliable and inter-comparable even though the IEC specifications are not fully satisfied.

On the other hand, requirements such as greater sensitivity/ low SNR for PD detection alone (without quantification in terms of pC) may be achieved through wideband sensors measuring over several tens of MHz. However, these measured values in mV pertain only to the specific setup (network configuration in this case) and cannot be translated to the charge value of the discharge which reflects the severity of the defect. Nevertheless, these methods are useful for continuous online PD monitoring to look at the development/progression of various discharge sources on critical network components.

Acknowledgements

The research was carried out at the UDEX Laboratory of Ormazabal Corporate Technology with funding from the transnational access activity of the ERIGrid project, a European Union Horizon 2020 Research and Innovation Programme (Grant Agreement N^o. 654113).



REFERENCES

- [1] IEC 62478, "High Voltage Test Techniques- Measurement of Partial Discharges by Electromagnetic and Acoustic Methods", 2016.
- [2] S.Boggs, A.Pathak and P.Walker, "Partial discharge. XXII. High frequency attenuation in shielded solid dielectric power cable and implications thereof for PD location," in *IEEE Electrical Insulation Magazine*, vol. 12, no. 1, pp. 9-16, Jan.-Feb. 1996.
- [3] Flexible RG58 Coax cable Datasheet, <https://www.pasternack.com/images/ProductPDF/RG58C-U.pdf>
- [4] R. Papazyan, P. Pettersson, H. Edin, R. Eriksson and U. Gafvert, "Extraction of high frequency power cable characteristics from S-parameter measurements," in *IEEE Transactions on Dielectrics and Electrical Insulation*, vol. 11, no. 3, pp. 461-470, June 2004.
- [5] Mugala, Gavita, et al. "Measurement technique for high frequency characterization of semiconducting materials in extruded cables." *IEEE transactions on dielectrics and electrical insulation* 11.3 (2004): 471-480.
- [6] IEC 60270, "High-voltage test techniques – Partial discharge measurement", 2015.
- [7] W.Hauschild, and E.Lemke. "High-voltage test and measuring techniques," *Heidelberg: Springer*, 2014.

Global Presence



Europe

HAEFELY AG
Birsstrasse 300
4052 Basel
Switzerland

 + 41 61 373 4111
 sales@haefely.com

China

HAEFELY AG Representative Office
8-1-602, Fortune Street, No. 67
Chaoyang Road, Beijing 100025
China

 + 86 10 8578 8099
 sales@haefely.com.cn

The original version of this article was published in the 25th International Conference on Electricity Distribution (CIRED), Madrid, 3-6 June 2019.

This is the author's pre-print version.